PRL **101,** 122301 (2008) PHYSICAL REVIEW LETTERS week ending 19 SEPTEMBER 2008

J/ψ Production in $\sqrt{s_{NN}} = 200$ GeV Cu + Cu Collisions

A. Adare,[8] S. Afanasiev,[22] C. Aidala,[9] N. N. Ajitanand,[48] Y. Akiba,[42,43] H. Al-Bataineh,[37] J. Alexander,[48] K. Aoki,[27,42] L. Aphecetche,[50] R. Armendariz,[37] S. H. Aronson,[3] J. Asai,[43] E. T. Atomssa,[28] R. Averbeck,[49] T. C. Awes,[38] B. Azmoun,[3] V. Babintsev,[18] G. Baksay,[14] L. Baksay,[14] A. Baldisseri,[11] K. N. Barish,[4] P. D. Barnes,[30] B. Bassalleck,[36] S. Bathe,[4] S. Batsouli,[38] V. Baublis,[41] A. Bazilevsky,[3] S. Belikov,[3,*] R. Bennett,[49] Y. Berdnikov,[45] A. A. Bickley,[8] J. G. Boissevain,[30] H. Borel,[11] K. Boyle,[49] M. L. Brooks,[30] H. Buesching,[3] V. Bumazhnov,[18] G. Bunce,[3,43] S. Butsyk,[30,49] S. Campbell,[49] B. S. Chang,[57] J.-L. Charvet,[11] S. Chernichenko,[18] J. Chiba,[23] C. Y. Chi,[9] M. Chiu,[19] I. J. Choi,[57] T. Chujo,[54] P. Chung,[48] A. Churyn,[18] V. Cianciolo,[38] C. R. Cleven,[16] B. A. Cole,[9] M. P. Comets,[39] P. Constantin,[30] M. Csanád,[13] T. Csörgő,[24] T. Dahms,[49] K. Das,[15] G. David,[3] M. B. Deaton,[1] K. Dehmelt,[14] H. Delagrange,[50] A. Denisov,[18] D. d'Enterria,[9] A. Deshpande,[43,49] E. J. Desmond,[3] O. Dietzsch,[46] A. Dion,[49] M. Donadelli,[46] O. Drapier,[28] A. Drees,[49] A. K. Dubey,[56] A. Durum,[18] V. Dzhordzhadze,[4] Y. V. Efremenko,[38] J. Egdemir,[49] F. Ellinghaus,[8] W. S. Emam,[4] A. Enokizono,[29] H. En'yo,[42,43] S. Esumi,[53] K. O. Eyser,[4] D. E. Fields,[36,43] M. Finger,[5,22] M. Finger, Jr.,[5,22] F. Fleuret,[28] S. L. Fokin,[26] Z. Fraenkel,[56,*] J. E. Frantz,[49] A. Franz,[3] A. D. Frawley,[15] K. Fujiwara,[42] Y. Fukao,[27,42] T. Fusayasu,[35] S. Gadrat,[31] I. Garishvili,[51] A. Glenn,[8] H. Gong,[49] M. Gonin,[28] J. Gosset,[11] Y. Goto,[42,43] R. Granier de Cassagnac,[28] N. Grau,[21] S. V. Greene,[54] M. Grosse Perdekamp,[19,43] T. Gunji,[7] H.-Å. Gustafsson,[32] T. Hachiya,[17] A. Hadj Henni,[50] C. Haegemann,[36] J. S. Haggerty,[3] H. Hamagaki,[7] R. Han,[40] H. Harada,[17] E. P. Hartouni,[29] K. Haruna,[17] E. Haslum,[32] R. Hayano,[7] M. Heffner,[29] T. K. Hemmick,[49] T. Hester,[4] X. He,[16] H. Hiejima,[19] J. C. Hill,[21] R. Hobbs,[36] M. Hohlmann,[14] W. Holzmann,[48] K. Homma,[17] B. Hong,[25] T. Horaguchi,[42,52] D. Hornback,[51] T. Ichihara,[42,43] K. Imai,[27,42] M. Inaba,[53] Y. Inoue,[44,42] D. Isenhower,[1] L. Isenhower,[1] M. Ishihara,[42] T. Isobe,[7] M. Issah,[48] A. Isupov,[22] B. V. Jacak,[49,+] J. Jia,[9] J. Jin,[9] O. Jinnouchi,[43] B. M. Johnson,[3] K. S. Joo,[34] D. Jouan,[39] F. Kajihara,[7] S. Kametani,[7,55] N. Kamihara,[42] J. Kamin,[49] M. Kaneta,[43] J. H. Kang,[57] H. Kanou,[42,52] D. Kawall,[43] A. V. Kazantsev,[26] A. Khanzadeev,[41] J. Kikuchi,[55] D. H. Kim,[34] D. J. Kim,[57] E. Kim,[47] E. Kinney,[8] A. Kiss,[13] E. Kistenev,[3] A. Kiyomichi,[42] J. Klay,[29] C. Klein-Boesing,[33] L. Kochenda,[41] V. Kochetkov,[18] B. Komkov,[41] M. Konno,[53] D. Kotchetkov,[4] A. Kozlov,[56] A. Král,[10] A. Kravitz,[9] J. Kubart,[5,20] G. J. Kunde,[30] N. Kurihara,[7] K. Kurita,[44,42] M. J. Kweon,[25] Y. Kwon,[51,57] G. S. Kyle,[37] R. Lacey,[48] Y.-S. Lai,[9] J. G. Lajoie,[21] A. Lebedev,[21] D. M. Lee,[30] M. K. Lee,[57] T. Lee,[47] M. J. Leitch,[30] M. A. L. Leite,[46] B. Lenzi,[46] T. Liška,[10] A. Litvinenko,[22] M. X. Liu,[30] X. Li,[6] B. Love,[54] D. Lynch,[3] C. F. Maguire,[54] Y. I. Makdisi,[3] A. Malakhov,[22] M. D. Malik,[36] V. I. Manko,[26] Y. Mao,[40,42] L. Mašek,[5,20] H. Masui,[53] F. Matathias,[9] M. McCumber,[49] P. L. McGaughey,[30] Y. Miake,[53] P. Mikeš,[5,20] K. Miki,[53] T. E. Miller,[54] A. Milov,[49] S. Mioduszewski,[3] M. Mishra,[2] J. T. Mitchell,[3] M. Mitrovski,[48] A. Morreale,[4] D. P. Morrison,[3] T. V. Moukhanova,[26] D. Mukhopadhyay,[54] J. Murata,[44,42] S. Nagamiya,[23] Y. Nagata,[53] J. L. Nagle,[8] M. Naglis,[56] I. Nakagawa,[42,43] Y. Nakamiya,[17] T. Nakamura,[17] K. Nakano,[42,52] J. Newby,[29] M. Nguyen,[49] B. E. Norman,[30] A. S. Nyanin,[26] E. O'Brien,[3] S. X. Oda,[7] C. A. Ogilvie,[21] H. Ohnishi,[42] H. Okada,[27,42] K. Okada,[43] M. Oka,[53] O. O. Omiwade,[1] A. Oskarsson,[32] M. Ouchida,[17] K. Ozawa,[7] R. Pak,[3] D. Pal,[54] A. P. T. Palounek,[30] V. Pantuev,[49] V. Papavassiliou,[37] J. Park,[47] W. J. Park,[25] S. F. Pate,[37] H. Pei,[21] J.-C. Peng,[19] H. Pereira,[11] V. Peresedov,[22] D. Yu. Peressounko,[26] C. Pinkenburg,[3] M. L. Purschke,[3] A. K. Purwar,[30] H. Qu,[16] J. Rak,[36] A. Rakotozafindrabe,[28] I. Ravinovich,[56] K. F. Read,[38,51] S. Rembeczki,[14] M. Reuter,[49] K. Reygers,[33] V. Riabov,[41] Y. Riabov,[41] G. Roche,[31] A. Romana,[28,*] M. Rosati,[21] S. S. E. Rosendahl,[32] P. Rosnet,[31] P. Rukoyatkin,[22] V. L. Rykov,[42] B. Sahlmueller,[33] N. Saito,[27,42,43] T. Sakaguchi,[3] S. Sakai,[53] H. Sakata,[17] V. Samsonov,[41] S. Sato,[23] S. Sawada,[23] J. Seele,[8] R. Seidl,[19] V. Semenov,[18] R. Seto,[4] D. Sharma,[56] I. Shein,[18] A. Shevel,[41,48] T.-A. Shibata,[42,52] K. Shigaki,[17] M. Shimomura,[53] K. Shoji,[27,42] A. Sickles,[49] C. L. Silva,[46] D. Silvermyr,[38] C. Silvestre,[11] K. S. Sim,[25] C. P. Singh,[2] V. Singh,[2] S. Skutnik,[21] M. Slunečka,[5,22] A. Soldatov,[18] R. A. Soltz,[29] W. E. Sondheim,[30] S. P. Sorensen,[51] I. V. Sourikova,[3] F. Staley,[11] P. W. Stankus,[38] E. Stenlund,[32] M. Stepanov,[37] A. Ster,[24] S. P. Stoll,[3] T. Sugitate,[17] C. Suire,[39] J. Sziklai,[24] T. Tabaru,[43] S. Takagi,[53] E. M. Takagui,[46] A. Taketani,[42,43] Y. Tanaka,[35] K. Tanida,[42,43] M. J. Tannenbaum,[3] A. Taranenko,[48] P. Tarján,[12] T. L. Thomas,[36] M. Togawa,[27,42] A. Toia,[49] J. Tojo,[42] L. Tomášek,[20] H. Torii,[42] R. S. Towell,[1] V-N. Tram,[28] I. Tserruya,[56] Y. Tsuchimoto,[17] C. Vale,[21] H. Valle,[54] H. W. van Hecke,[30] J. Velkovska,[54] R. Vertesi,[12] A. A. Vinogradov,[26] M. Virius,[10] V. Vrba,[20] E. Vznuzdaev,[41] M. Wagner,[27,42] D. Walker,[49] X. R. Wang,[37] Y. Watanabe,[42,43] J. Wessels,[33] S. N. White,[3] D. Winter,[9] C. L. Woody,[3] M. Wysocki,[8] W. Xie,[43] Y. L. Yamaguchi,[55] A. Yanovich,[18] Z. Yasin,[4] J. Ying,[16] S. Yokkaichi,[42,43] G. R. Young,[38] I. Younus,[36] I. E. Yushmanov,[26] W. A. Zajc,[9] O. Zaudtke,[33] C. Zhang,[38] S. Zhou,[6] J. Zimányi,[24,*] and L. Zolin[22]

(PHENIX Collaboration)

0031-9007/08/101(12)/122301(6)

[1]*Abilene Christian University, Abilene, Texas 79699, USA*
[2]*Department of Physics, Banaras Hindu University, Varanasi 221005, India*
[3]*Brookhaven National Laboratory, Upton, New York 11973-5000, USA*
[4]*University of California-Riverside, Riverside, California 92521, USA*
[5]*Charles University, Ovocný trh 5, Praha 1, 116 36, Prague, Czech Republic*
[6]*China Institute of Atomic Energy (CIAE), Beijing, People's Republic of China*
[7]*Center for Nuclear Study, Graduate School of Science, University of Tokyo, 7-3-1 Hongo, Bunkyo, Tokyo 113-0033, Japan*
[8]*University of Colorado, Boulder, Colorado 80309, USA*
[9]*Columbia University, New York, New York 10027*
and Nevis Laboratories, Irvington, New York 10533, USA
[10]*Czech Technical University, Zikova 4, 166 36 Prague 6, Czech Republic*
[11]*Dapnia, CEA Saclay, F-91191, Gif-sur-Yvette, France*
[12]*Debrecen University, H-4010 Debrecen, Egyetem tér 1, Hungary*
[13]*ELTE, Eötvös Loránd University, H-1117 Budapest, Pázmány P. s. 1/A, Hungary*
[14]*Florida Institute of Technology, Melbourne, Florida 32901, USA*
[15]*Florida State University, Tallahassee, Florida 32306, USA*
[16]*Georgia State University, Atlanta, Georgia 30303, USA*
[17]*Hiroshima University, Kagamiyama, Higashi-Hiroshima 739-8526, Japan*
[18]*IHEP Protvino, State Research Center of Russian Federation, Institute for High Energy Physics, Protvino, 142281, Russia*
[19]*University of Illinois at Urbana-Champaign, Urbana, Illinois 61801, USA*
[20]*Institute of Physics, Academy of Sciences of the Czech Republic, Na Slovance 2, 182 21 Prague 8, Czech Republic*
[21]*Iowa State University, Ames, Iowa 50011, USA*
[22]*Joint Institute for Nuclear Research, 141980 Dubna, Moscow Region, Russia*
[23]*KEK, High Energy Accelerator Research Organization, Tsukuba, Ibaraki 305-0801, Japan*
[24]*KFKI Research Institute for Particle and Nuclear Physics of the Hungarian Academy of Sciences (MTA KFKI RMKI),*
H-1525 Budapest 114, POBox 49, Budapest, Hungary
[25]*Korea University, Seoul, 136-701, Korea*
[26]*Russian Research Center "Kurchatov Institute", Moscow, Russia*
[27]*Kyoto University, Kyoto 606-8502, Japan*
[28]*Laboratoire Leprince-Ringuet, Ecole Polytechnique, CNRS-IN2P3, Route de Saclay, F-91128, Palaiseau, France*
[29]*Lawrence Livermore National Laboratory, Livermore, California 94550, USA*
[30]*Los Alamos National Laboratory, Los Alamos, New Mexico 87545, USA*
[31]*LPC, Université Blaise Pascal, CNRS-IN2P3, Clermont-Fd, 63177 Aubiere Cedex, France*
[32]*Department of Physics, Lund University, Box 118, SE-221 00 Lund, Sweden*
[33]*Institut für Kernphysik, University of Muenster, D-48149 Muenster, Germany*
[34]*Myongji University, Yongin, Kyonggido 449-728, Korea*
[35]*Nagasaki Institute of Applied Science, Nagasaki-shi, Nagasaki 851-0193, Japan*
[36]*University of New Mexico, Albuquerque, New Mexico 87131, USA*
[37]*New Mexico State University, Las Cruces, New Mexico 88003, USA*
[38]*Oak Ridge National Laboratory, Oak Ridge, Tennessee 37831, USA*
[39]*IPN-Orsay, Universite Paris Sud, CNRS-IN2P3, BP1, F-91406, Orsay, France*
[40]*Peking University, Beijing, People's Republic of China*
[41]*PNPI, Petersburg Nuclear Physics Institute, Gatchina, Leningrad region, 188300, Russia*
[42]*RIKEN, The Institute of Physical and Chemical Research, Wako, Saitama 351-0198, Japan*
[43]*RIKEN BNL Research Center, Brookhaven National Laboratory, Upton, New York 11973-5000, USA*
[44]*Physics Department, Rikkyo University, 3-34-1 Nishi-Ikebukuro, Toshima, Tokyo 171-8501, Japan*
[45]*Saint Petersburg State Polytechnic University, St. Petersburg, Russia*
[46]*Universidade de São Paulo, Instituto de Física, Caixa Postal 66318, São Paulo CEP05315-970, Brazil*
[47]*System Electronics Laboratory, Seoul National University, Seoul, Korea*
[48]*Chemistry Department, Stony Brook University, SUNY, Stony Brook, New York 11794-3400, USA*
[49]*Department of Physics and Astronomy, Stony Brook University, SUNY, Stony Brook, New York 11794, USA*
[50]*SUBATECH (Ecole des Mines de Nantes, CNRS-IN2P3, Université de Nantes) BP 20722-44307, Nantes, France*
[51]*University of Tennessee, Knoxville, Tennessee 37996, USA*
[52]*Department of Physics, Tokyo Institute of Technology, Oh-okayama, Meguro, Tokyo 152-8551, Japan*
[53]*Institute of Physics, University of Tsukuba, Tsukuba, Ibaraki 305, Japan*
[54]*Vanderbilt University, Nashville, Tennessee 37235, USA*
[55]*Waseda University, Advanced Research Institute for Science and Engineering, 17 Kikui-cho, Shinjuku-ku, Tokyo 162-0044, Japan*
[56]*Weizmann Institute, Rehovot 76100, Israel*
[57]*Yonsei University, IPAP, Seoul 120-749, Korea*

(Received 31 December 2007; published 18 September 2008)

Yields for J/ψ production in Cu + Cu collisions at $\sqrt{s_{NN}} = 200$ GeV have been measured over the rapidity range $|y| < 2.2$ and compared with results in $p + p$ and Au + Au collisions at the same energy. The Cu + Cu data offer greatly improved precision over existing Au + Au data for J/ψ production in collisions with small to intermediate numbers of participants, in the range where the quark-gluon plasma transition threshold is predicted to lie. Cold nuclear matter estimates based on *ad hoc* fits to d + Au data describe the Cu + Cu data up to $N_{\text{part}} \sim 50$, corresponding to a Bjorken energy density of at least 1.5 GeV/fm^3.

DOI: 10.1103/PhysRevLett.101.122301 PACS numbers: 25.75.Dw

High-energy heavy-ion collisions provide the opportunity to study strongly interacting matter at very high-energy densities where quantum chromodynamics (QCD) predicts a transition from normal nuclear matter to a deconfined system of quarks and gluons, the quark-gluon plasma (QGP) [1]. At the Relativistic Heavy Ion Collider (RHIC) the energy density in central Au + Au collisions is well in excess of the critical energy density expected for this transition [2].

Over the past 20 years, there has been intense theoretical and experimental work on J/ψ production. First predicted by Matsui and Satz [3], suppression of quarkonia production in ultrarelativistic heavy-ion collisions was expected to be an unambiguous signature for the formation of a QGP. It is now recognized that in order to interpret J/ψ production as a QGP probe one has to consider cold nuclear matter effects such as initial state energy loss [4] and shadowing [5], as well as charm quark energy loss [6], comover interactions [7], corrections for feed-down from higher mass charmonium states, and secondary production mechanisms, such as recombination of initially uncorrelated $c\bar{c}$ pairs [8].

Experiment NA50 reported suppression of J/ψ production in Pb + Pb collisions at $\sqrt{s_{NN}} = 17.3$ GeV [9] that exceeds expectations based on their measurements of cold nuclear matter effects in $p + A$ collisions [10]. NA60 observed similar behavior in In + In collisions at the same energy [11]. The PHENIX experiment [12] at RHIC has characterized effects of the nuclear medium on J/ψ production at $\sqrt{s_{NN}} = 200$ GeV. The basic invariant yield reference is obtained from $p + p$ data [13–15]. Cold nuclear matter effects are studied using d + Au data [14,16]. Cold and hot nuclear matter effects are studied for large numbers of participants (N_{part}) using Au + Au data [17,18], and for smaller N_{part} using Cu + Cu data, the subject of this Letter. The results are presented as a nuclear modification factor, R_{AA}, the ratio of the yield in heavy-ion collisions to the yield in $p + p$ collisions scaled by the number of binary nucleon-nucleon collisions (N_{coll}), which is appropriate for pointlike processes.

Lattice QCD calculations [19] indicate that the threshold energy density for QGP formation is of order 1 GeV/fm^3. At $\sqrt{s_{NN}} = 200$ GeV this is expected to occur below $N_{\text{part}} = 100$ [20], in a region where Au + Au data have limited statistical and systematic precision [18]. High statistics measurements with the intermediate sized system Cu + Cu provide crucial information in that important region.

In this Letter we present results obtained by PHENIX during the 2005 RHIC run on the production of J/ψ in Cu + Cu collisions at $\sqrt{s_{NN}} = 200$ GeV. J/ψ invariant yields were studied via $J/\psi \to e^+e^-$ decays measured at midrapidity with the central arm spectrometers ($|y| \leq 0.35$, $\Delta\phi = 2 \times 90°$), and $J/\psi \to \mu^+\mu^-$ decays measured at forward rapidity with the two muon arm spectrometers ($1.2 < |y| < 2.2$, $\Delta\phi = 360°$). Event centrality and the location of the collision vertex along the beam axis (z_{vtx}) are measured with two Beam-Beam Counters (BBC) located at $3.0 < |\eta| < 3.9$. A Glauber model and a simulation of the BBC response was used to determine N_{part} and N_{coll} and their systematic uncertainties for different collision centrality ranges [21].

Data were recorded using lepton triggers in coincidence with a minimum bias trigger which required a coincidence between the BBC detectors and a valid z_{vtx}. After applying a cut of $|z_{vtx}| < 30$ cm and quality assurance criteria, the data correspond to a sampled luminosity of about 2.1 nb^{-1} (1.3 nb^{-1}) in the e^+e^- ($\mu^+\mu^-$) analysis.

Electron detection at midrapidity used the drift chambers for momentum measurement, the pad chambers for pattern recognition and track location, and the ring imaging Cherenkov (RICH) detector plus electromagnetic calorimeter (EMCal) for electron identification. Charged particle tracks were matched with a RICH ring and an EMCal hit to select electron candidates by requiring at least two RICH phototube hits inside an annulus around the projected ring center, ring quality cuts, track or cluster position matching cuts at the EMCal, and a cut on the ratio of EMCal energy to track momentum, $E/p - \langle E/p \rangle > -2\sigma$.

The $J/\psi \to e^+e^-$ trigger required one signal above a certain energy threshold in the EMCal and a matching RICH hit. Two energy thresholds were used during the run, 1.1 and 0.8 GeV, yielding average J/ψ trigger efficiencies of ~65% and 82%, respectively. The $J/\psi \to e^+e^-$ signal extraction method was very similar to the method used in the recent Au + Au [18] and $p + p$ [15] analyses. The like sign invariant mass spectrum was subtracted from the unlike sign spectrum. The remaining yield in the J/ψ mass region ($2.9 \leq M_{\text{inv}} \leq 3.3$ GeV/c^2) was corrected for pairs lost to the radiative tail and pairs added by the continuum signal under the peak [15]. The total J/ψ count in the e^+e^- channel was ≈ 2050. The signal to background ratio (S/B) was ≈ 1(6) for the most central (peripheral) collisions.

Muon detection at forward and backward rapidities used the muon arms, consisting of cathode strip tracking chambers in a magnetic field (MuTr) and Iarocci tube planes interleaved with thick steel absorbers (MuID). Muon candidates were identified by penetration to the last MuID gap, and their momenta were measured by their bend through the MuTr.

The dimuon trigger required two candidate tracks to penetrate the MuID, point back to the event vertex, and pass an opening angle cut ($\theta > 19°$). The dimuon combinatorial background was estimated using the product of the like sign counts, $2\sqrt{N^{++}N^{--}}$, and was subtracted from the unlike sign spectra. The residual background (notably from the open charm pairs and Drell-Yan processes) was evaluated using an exponential form. The $J/\psi \rightarrow \mu^+\mu^-$ signal was estimated by direct counting of the remaining pairs above the exponential fit in the mass range $2.6 \leq M_{\rm inv} \leq 3.6$ GeV$/c^2$ and also by using two fits with different parameterizations (single and double Gaussian) of the J/ψ line shapes, as described in [15,18]. The average of the results gave the signal count and the variation gave the systematic error. The total J/ψ yield was ≈ 9000. The S/B was ≈ 0.3(1.0) for the most central(peripheral) collisions.

The J/ψ invariant yield in the appropriate centrality, rapidity, and transverse momentum bin is given by

$$\frac{B_{ll}}{2\pi p_T}\frac{d^2N_{J/\psi}}{dp_T dy} = \frac{1}{2\pi p_T}\frac{N_{J/\psi}}{N_{\rm evt}\Delta y \Delta p_T A\varepsilon}, \qquad (1)$$

with B_{ll} the branching ratio for $J/\psi \rightarrow l^+l^-$, $N_{J/\psi}$ the number of observed J/ψ, $N_{\rm evt}$ the number of events; Δy the rapidity range; Δp_T the transverse momentum range, and $A\varepsilon$ the acceptance and efficiency correction (including trigger efficiency).

The determination of $A\varepsilon$ is done with a full GEANT simulation. The method is described in more detail in [15]. $A\varepsilon$ decreases with the collision centrality due to overlapping hits in the RICH and the EMCal in the central arm, and in the MuTr for the forward arms, leading to an increasing fraction of misreconstructed tracks in higher multiplicity events. This effect is evaluated by embedding simulated single J/ψ events in real events. The efficiency loss in the most central collisions is 3% for dielectron measurements and 20% (16%) for dimuon measurements at positive (negative) rapidity.

Systematic uncertainties in the measured J/ψ invariant yield depend on J/ψ rapidity and transverse momentum as well as on event centrality. Systematic uncertainties are grouped into three categories: point to point uncorrelated uncertainties (type A), which can move the points independently of each other, point to point correlated uncertainties (type B), which can move the points coherently, though not necessarily by the same amount, and global systematic uncertainties (type C). In all plots point to point uncorrelated systematic uncertainties and statistical uncertainties are quadratically summed and represented by vertical bars, point to point correlated systematic uncertainties are represented by boxes, and global systematic uncertainties (if any) are quoted.

TABLE I. Systematic error sources, values, and types for R_{AA} vs $N_{\rm part}$ in the two rapidity intervals. Where a range is given, it is from peripheral to central collisions.

Source	$\vert y\vert < 0.3$	$\vert y\vert \in [1.2, 2.2]$	Type
Signal extraction	6%	5%–6%	A
Detector + trigger efficiency	1.4%–5%	3%	B
Run by run variation	5%	2%	B
Input $y + p_T$ distributions	2%	3%	B
$N_{\rm coll}$	14%–11%	14%–11%	B

Systematic uncertainties of type A and B for R_{AA} vs $N_{\rm part}$ are summarized in Table I. Some uncertainties in the invariant yield, such as that on the acceptance, cancel out for R_{AA} and are not shown. Global systematic uncertainties for R_{AA} vs $N_{\rm part}$ include the $p + p$ J/ψ yield uncertainty and some $p + p$ systematic errors that do not cancel when forming R_{AA}.

Results for the two muon arms agree within uncertainties and are combined where appropriate. Figure 1 shows the J/ψ yield vs p_T for different Cu + Cu centrality classes at mid and forward rapidity. As was done previously for the Au + Au case [18], the mean square transverse momentum, $\langle p_T^2\rangle$, was calculated numerically from the data for $p_T < 5$ GeV$/c$. The Cu + Cu data are plotted vs $N_{\rm part}$ and compared with the corresponding values from

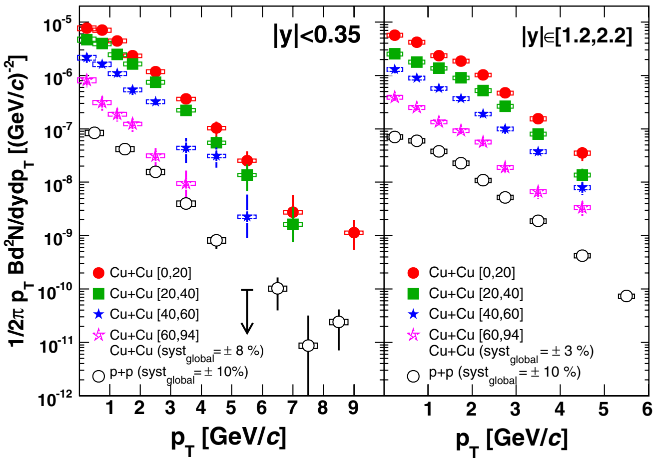

FIG. 1 (color online). J/ψ yield vs p_T at mid (left) and forward (right) rapidity for different Cu + Cu centrality bins and for $p + p$ [15]. Uncertainties are described in the text.

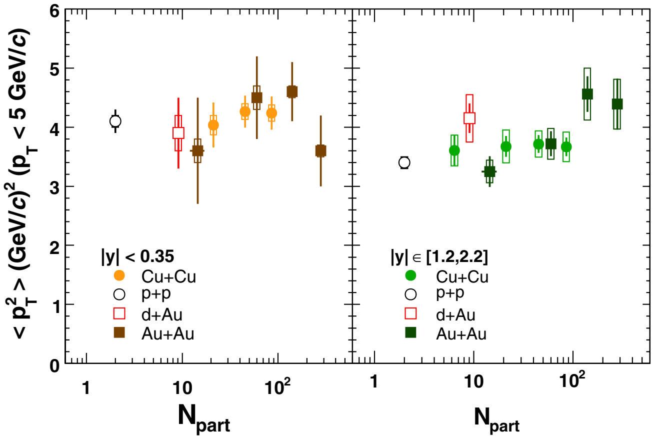

FIG. 2 (color online). The $\langle p_T^2 \rangle$ vs $N_{\rm part}$ for J/ψ production in Cu + Cu, $p + p$ [15], d + Au [16] and Au + Au [18] collisions at mid (left) and forward (right) rapidity.

Au + Au [18], d + Au [16] and $p + p$ [15] collisions in Fig. 2. Within uncertainties, the data for Cu + Cu and Au + Au agree where they overlap in $N_{\rm part}$, and the $\langle p_T^2 \rangle$ for the Cu + Cu data seems independent of $N_{\rm part}$.

The R_{AA} values vs p_T and rapidity are shown in Fig. 3 for the 0–20% most central Cu + Cu collisions. We see similar behavior for mid and forward rapidity, and there appears to be no p_T dependence in all centrality classes. The rms width of the rapidity distribution (evaluated directly from the data) is identical, within ~2–3% uncertainties, in $p + p$ collisions and in all centrality classes for Cu + Cu collisions.

Figures 4(a) and 4(b) show similar behavior within uncertainties for R_{AA} in Cu + Cu and Au + Au [18] collisions at comparable values of $N_{\rm part}$. Theoretical calculations [22] including only modified initial parton distribution functions and an added $J/\psi - N$ breakup cross section were fitted in [16] to d + Au J/ψ R_{AA} data. The EKS98 [23,24] and nDSg [25] shadowing models were used. The fit was made simultaneously to all rapidities by optimizing the breakup cross section. While consistent with the low statistics d + Au data [16], this method leads to a model dependence of the CNM effects, since the rapidity shape is determined entirely by the shadowing model. In an attempt to reduce this model dependence, we used a data-driven *ad hoc* model to parameterize the d + Au data [16]. The *ad hoc* model uses EKS98 (method 1) and nDSg (method 2) shadowing parameterizations for the relative rapidity dependence within the fitted rapidity ranges, but the breakup cross section is replaced with a quantity, which we call f, that is optimized separately for $y = 0$ and $|y| = 1.7$. The fits using method 1 yielded $f_{dAu} = 2.3 \pm^{2.1}_{1.6}$ mb at $y = 0$ and $3.9 \pm^{1.3}_{1.2}$ mb at $|y| = 1.7$. The method 2 fits yielded $f_{dAu} = 0.9 \pm^{1.9}_{1.8}$ mb at $y = 0$ and $3.3 \pm^{1.3}_{1.2}$ mb at $|y| = 1.7$. The resulting separate parameterizations of the d + Au data vs $N_{\rm coll}$ at mid and forward/backward rapidity can be projected to Cu + Cu and Au + Au using the corresponding parton distribution functions for Cu and Au [22]. The results for method 1 are shown in Fig. 4 as cold nuclear matter baseline R_{AA} curves

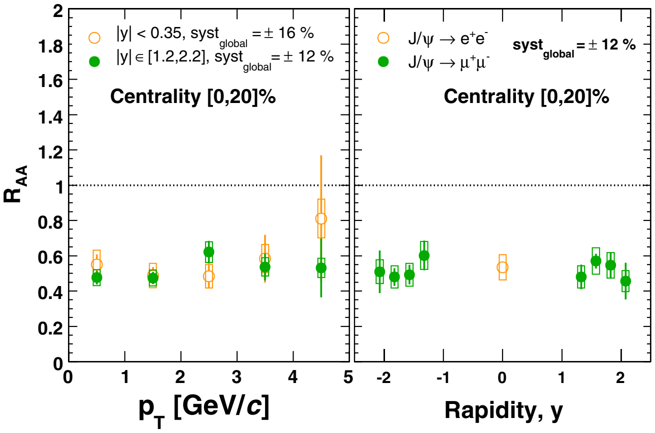

FIG. 3 (color online). R_{AA} vs p_T (left) and y (right) for J/ψ production in the most central Cu + Cu collisions.

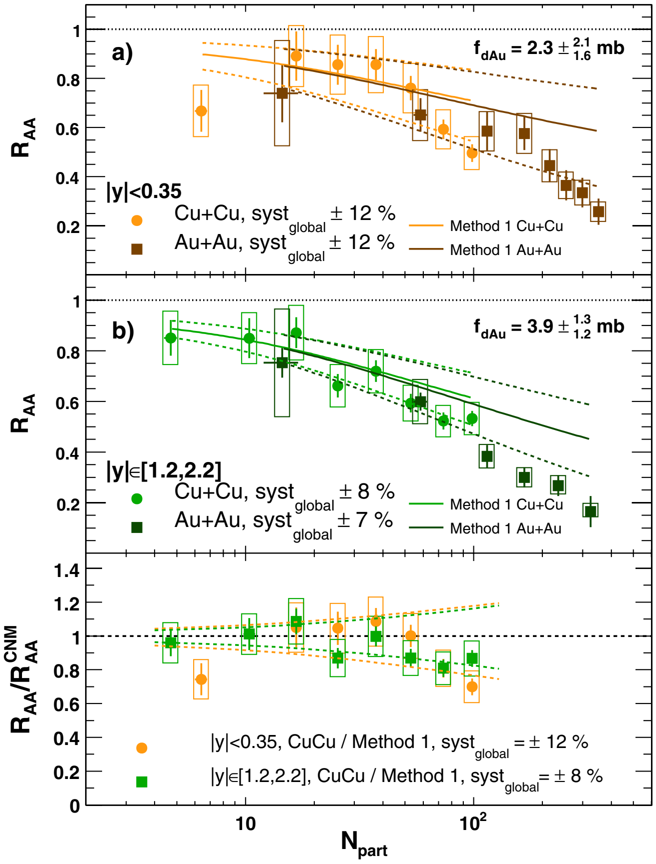

FIG. 4 (color online). (a),(b) R_{AA} vs $N_{\rm part}$ for J/ψ production in Cu + Cu and Au + Au [18] collisions. The curves are predictions from *ad hoc* fits to d + Au data [16] and are discussed in the text. (c) Ratios of the measured R_{AA} values to the predicted cold nuclear matter R_{AA}. The dashed lines show the 1σ uncertainties from the d + Au fits.

calculated from the best fit values of f (solid lines) and the 1 standard deviation uncertainty in f (dashed lines). The method 2 heavy-ion calculations are similar to those from method 1, leading to very similar conclusions, and are not shown in Fig. 4. In Fig. 4(c) the measured R_{AA} values for Cu + Cu are shown divided by the method 1 calculations for Cu + Cu. The Cu + Cu R_{AA} is seen to be consistent with the cold nuclear matter projection within about 15% uncertainties up to $N_{\rm part} \sim 50$. Given the uncertainty in the cold nuclear matter reference at larger $N_{\rm part}$ values, we can not currently draw any strong conclusions there. However PHENIX completed in February 2008 a second d + Au run, with approximately 30 times the statistics of the first d + Au run in 2003. With the new reference d + Au data, we expect to be able to identify if and where the measured Cu + Cu R_{AA} departs from the cold nuclear matter baseline.

In summary, we present high statistics J/ψ data from Cu + Cu collisions at RHIC, providing for the first time detailed information on R_{AA} and $\langle p_T^2 \rangle$ for $N_{\rm part} < 100$. The rms values of the rapidity distributions at all centralities are consistent with that for $p + p$, and the measured $\langle p_T^2 \rangle$ for $p_T < 5$ GeV/c is nearly independent of centrality and rapidity. At similar values of $N_{\rm part}$, R_{AA} and $\langle p_T^2 \rangle$ are found to agree within errors for Cu + Cu and Au + Au collisions. Cold nuclear matter calculations based on *ad hoc* fits to d + Au data reproduce the peripheral Cu + Cu data well up to $N_{\rm part} \sim 50$, corresponding to $\epsilon_{Bjorken}\tau \sim 1.5$ GeV/fm^2/c [20], where $\epsilon_{Bjorken}$ is the Bjorken energy density and τ is the formation time. For an estimate of the thermalized energy density, hydrodynamical models give thermalization times in the range of 0.6 fm/c to 1.0 fm/c [2], which implies that cold nuclear matter effects dominate J/ψ production up to thermalized energy densities of ~1.5 to 2.5 GeV/fm^3.

We thank the staff of the Collider-Accelerator and Physics Departments at BNL for their vital contributions. We acknowledge support from the Office of Nuclear Physics in DOE Office of Science and NSF (U.S.), MEXT and JSPS (Japan), CNPq and FAPESP (Brazil), NSFC (China), MSMT (Czech Republic), IN2P3/CNRS, and CEA (France), BMBF, DAAD, and AvH (Germany), OTKA (Hungary), DAE (India), ISF (Israel), KRF and KOSEF (Korea), MES, RAS, and FAAE (Russia), VR and KAW (Sweden), U.S. CRDF for the FSU, US-Hungarian NSF-OTKA-MTA, and US-Israel BSF.

---

[*] Deceased.

[+] PHENIX Spokesperson: jacak@skipper.physics.sunysb.edu

[1] J. W. Harris and B. Müller, Annu. Rev. Nucl. Part. Sci. **46**, 71 (1996).
[2] K. Adcox *et al.*, Nucl. Phys. **A757**, 184 (2005).
[3] T. Matsui and H. Satz, Phys. Lett. B **178**, 416 (1986).
[4] M. B. Johnson *et al.*, Phys. Rev. Lett. **86**, 4483 (2001).
[5] V. Guzey, M. Strikman, and W. Vogelsang, Phys. Lett. B **603**, 173 (2004).
[6] R. Baier, D. Schiff, and B. G. Zakharov, Annu. Rev. Nucl. Part. Sci. **50**, 37 (2000).
[7] S. Gavin and R. Vogt, Nucl. Phys. **A610**, 442c (1996).
[8] R. L. Thews and M. L. Mangano, Phys. Rev. C **73**, 014904 (2006).
[9] B. Alessandro *et al.*, Eur. Phys. J. C **39**, 335 (2005).
[10] B. Alessandro *et al.*, Eur. Phys. J. C **48**, 329 (2006).
[11] R. Arnaldi *et al.*, arXiv:0706.4361.
[12] K. Adcox *et al.*, Nucl. Instrum. Methods Phys. Res., Sect. A **499**, 469 (2003).
[13] S. S. Adler *et al.*, Phys. Rev. Lett. **92**, 051802 (2004).
[14] S. S. Adler *et al.*, Phys. Rev. Lett. **96**, 012304 (2006).
[15] A. Adare *et al.*, Phys. Rev. Lett. **98**, 232002 (2007).
[16] A. Adare *et al.*, Phys. Rev. C **77**, 024912 (2008).
[17] S. S. Adler *et al.*, Phys. Rev. C **69**, 014901 (2004).
[18] A. Adare *et al.*, Phys. Rev. Lett. **98**, 232301 (2007).
[19] F. Karsch, Lect. Notes Phys. **583**, 209 (2002).
[20] S. S. Adler *et al.*, Phys. Rev. C **71**, 034908 (2005).
[21] A. Adare *et al.*, arXiv:0801.4555.
[22] R. Vogt, Phys. Rev. C **71**, 054902 (2005).
[23] K. J. Eskola, V. J. Kolhinen, and P. V. Ruuskanen, Nucl. Phys. **B535**, 351 (1998).
[24] K. J. Eskola, V. J. Kolhinen, and C. A. Salgado, Eur. Phys. J. C **9**, 61 (1998).
[25] D. de Florian and R. Sassot, Phys. Rev. D **69**, 074028 (2004).